Cell Imaging

DOI: 10.1002/ange.201007979

Long-Term Real-Time Tracking of Lanthanide Ion Doped Upconverting Nanoparticles in Living Cells**

Sang Hwan Nam, Yun Mi Bae, Yong Il Park, Jeong Hyun Kim, Hyung Min Kim, Joon Sig Choi, Kang Taek Lee, Taeghwan Hyeon, and Yung Doug Suh**

Recently, there has been great interest in employing nanoparticles for various biological applications.[1] Nanoparticles can be synthesized in a controlled manner such that they have desirable sizes, shapes, and optical or magnetic properties. In addition, one may provide nanoparticles with biological functions through chemical surface modifications and conjugation of ligands.[2] Such intrinsic and extrinsic properties of nanoparticles enable them to be used as excellent biological imaging probes and diagnostic/therapeutic agents at the cellular level.[3] Among the various nanoparticle systems developed thus far, semiconductor nanocrystals or quantum dots (QDs) are most widely used. QDs are extremely bright and photostable, and exhibit excellent spectral properties (i.e., broad absorption and narrow emission bands) suited for multicolor detection.[4–6] However, the drawbacks such as photoblinking,[7] the presence of nonradiant dark particles,[8] and potential cytotoxicity[9] limit their applicability. In recent years, several alternative types of luminescent nanoparticles have been introduced for biological applications. For example, nanodiamonds (NDs) with nitrogen vacancy centers were found to be highly photoluminescent while exhibiting no photoblinking and photobleaching,[10,11] and even useful as the imaging probe for super-resolution optical microscopy.[12] However, applying NDs for biological imaging has limitations, especially in the case of long-term tracking studies, since the excitation in the blue or green region (typically 488 or 532 nm) might result in fatal photodamage to cells or low penetration depth into tissues. In contrast, single-walled carbon nanotubes (SWNTs) were shown to be appropriate for biological imaging in that the excitation and emission lie in the near-infrared (NIR) spectral range.[13–15] However, being longer than 100 nm typically, SWNTs are considered to be too large to be used as biolabels. Meanwhile, lanthanide ion doped upconverting nanoparticles (UCNPs), which emit in the visible range upon absorption of NIR photons, have attracted great attention owing to their unique optical properties. First, two-photon upconversion of NIR excitation to the emission of a visible photon is so efficient that a tiny continuous-wave (CW) diode laser (980 nm) with the output of tens of milliwatts is sufficient as the excitation source.[16,17] Second, by employing NIR excitation, one can suppress cellular autofluorescence, induce little photodamage to living cells, and achieve relatively deep penetration into tissues.[18,19] Finally, UCNPs exhibit neither photoblinking on the millisecond and second time scales nor photobleaching even with hours of continuous excitation,[20,21] their cytotoxicity is very low,[20,22] and the inclusion or doping of Gd^{3+} ions in the host materials endows UCNPs with an additional modality for magnetic resonance imaging (MRI).[20,23] As a result, UCNPs became one of the most promising nanoparticle systems for biological imaging and there are continuing efforts to improve their properties (e.g., increasing luminescence intensity and reducing the particle size) by designing new synthetic strategies.[24] Herein, we report the first real-time tracking study with UCNPs at the single vesicle level in living cells. Thanks to the remarkable photostability of UCNPs and the noninvasiveness of NIR excitation, we were able to visualize the intracellular movements of UCNPs for as long as 6 h without interruption.

We first assessed the benefits of using NIR radiation as the excitation source to demonstrate the feasibility of long-term live-cell imaging with UCNPs. The UCNPs (hexagonal-phase $NaYF_4$ co-doped with Yb^{3+} and Er^{3+}, ca. 30 nm in diameter) coated by amphiphilic PEG–phospholipids (PEG = poly(ethylene glycol)) were internalized into HeLa cells and imaged on a home-made epi-fluorescence microscope setup (Methods section and Figures S1 and S2 in the Supporting

[*] Dr. S. H. Nam,[+] Y. M. Bae,[+] Dr. H. M. Kim, Dr. K. T. Lee, Dr. Y. D. Suh
Laboratory for Advanced Molecular Probing (LAMP)
NanoBio Fusion Research Center, Korea Research Institute of Chemical Technology, Daejeon 305-600 (Korea)
Fax: (+82) 42-860-7164
E-mail: ktlee@krict.re.kr
ydsuh@krict.re.kr

Y. I. Park,[+] Dr. J. H. Kim, Prof. Dr. T. Hyeon
National Creative Research Initiative Center for Oxide Nanocrystalline Materials, World Class University (WCU) Program of Chemical Convergence for Energy & Environment (C2E2)
School of Chemical and Biological Engineering, Seoul National University, Seoul 151-744 (Korea)

Y. M. Bae,[+] Prof. Dr. J. S. Choi
Department of Biochemistry, Chungnam National University
Daejeon 305-764 (Korea)

[+] These authors contributed equally to this work.

[**] K.T.L. was supported by the Pioneer Research Center Program (2010-0002195) of NRF. Y.D.S. was supported by the Eco-technopia 21 Project by KME and the Development of Advanced Scientific Analysis Instrumentation Project of KRISS by MEST. K.T.L. and Y.D.S. also acknowledge support by the Nano R&D Program (2010-0019142, 2007-02843) of NRF, the Industrial Core Technology Development Program (10033183, 10037397) of MKE, and KRICT (KK-1004-B0, SI-1110). T.H. acknowledges financial support by the National Creative Research Initiative (R16-2002-003-01001-0), the Strategic Research (2010-0029138), and the World Class University (R31-10013) Programs of NRF. H.M.K. was supported by the Public Welfare & Safety Research Program (2010-0020-795) of NRF. Y.I.P. was supported by a Seoul Science Fellowship.

Supporting information for this article is available on the WWW under http://dx.doi.org/10.1002/anie.201007979.

Information). In Figure 1 a, we chose a single HeLa cell (left panel) with internalized UCNPs and obtained a luminescence image with 980 nm excitation (right panel). It is shown that the signal levels from the extracellular medium (1) and the

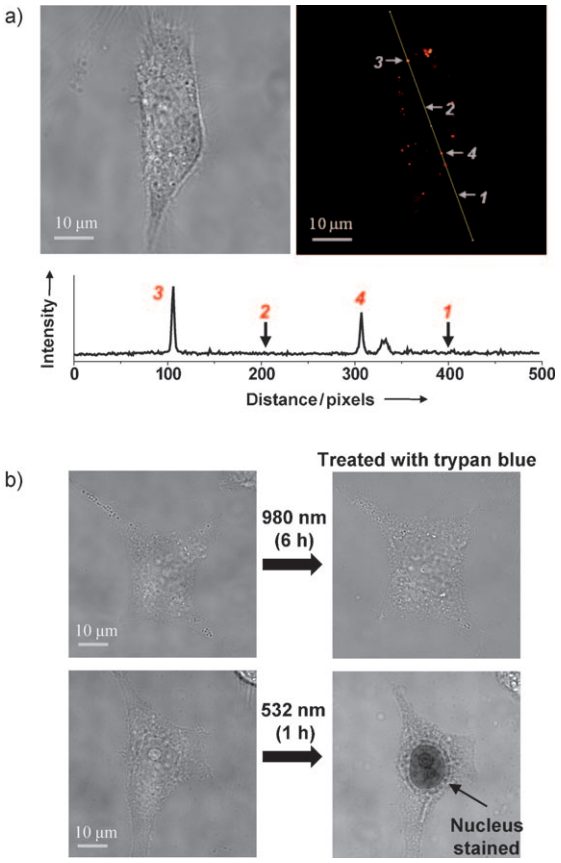

Figure 1. a) Bright-field (left) and luminescence (right) images of a single HeLa cell with internalized UCNPs, and intensity profile (bottom) along the line in the luminescence image. b) Bright-field images of single HeLa cells after continuous illumination by 980 nm (3 kW cm^{-2}, top) and 532 nm (1 W cm^{-2}, bottom) lasers for 6 h and 1 h, respectively.

cell body (2) are essentially indistinguishable. However, the luminescence signals from the UCNPs (3 and 4) inside the cell are significantly higher than the background. This clearly shows that cellular autofluorescence is totally absent with 980 nm excitation and the luminescence of UCNPs is intense enough to give very high image contrast. We also note that, even with relatively simple epi-fluorescence microscopy, one can achieve a signal-to-background ratio comparable to that of confocal microscopy because 980 nm excitation does not generate any out-of-focus background. At the same time, the merits of wide-field microscopy such as high temporal resolution can still be pursued. To further increase the signal level of UCNPs, one may raise the laser power for excitation. Usually, high laser power is accompanied by lethal photoinduced damage to the cells and thereby limits the time window for continuous observation. It is well known, however, that the optical absorption cross sections of cellular components are dramatically reduced in the NIR range,[25,26] and thus the chances of subsequent photoinduced damage upon NIR excitation are minimized. In fact, we found that 980 nm excitation is noninvasive to the living cells as expected. For example, even after illuminating a single HeLa cell for 6 h without interruption, the cell remained viable as manifested by the observation that trypan blue treatment did not stain the nucleus (Figure 1 b, upper panel). In contrast, when a different cell was illuminated with a visible laser (532 nm) for comparison, it was dead in 1 h even with a power of 1 W cm^{-2} (Figure 1 b, lower panel), which is two orders of magnitude lower than that of 980 nm excitation. Combined with the low cytotoxicity (Methods section and Figure S3 in the Supporting Information) and photostability of UCNPs, such advantages of NIR excitation, namely, the absence of autofluorescence and low degree of photodamage, allow long-term continuous observations of living cells.

Figure 2 shows snapshot images of UCNPs in a single living HeLa cell adopted from a real-time movie acquired continuously for 6 h at the frame rate of 20 frames s^{-1}. The UCNPs were internalized most probably by endocytosis, a ubiquitous pathway for cellular uptake of nanoparticles.[27–29] This should be nonspecific endocytosis, since there are no specific ligands on the particle surface that are supposed to bind receptors on the cell membrane. Given the typical size of UCNPs (ca. 40 nm with the PEG–phospholipid coating; Figure S1 in the Supporting Information), the relevant mechanism is likely to be pinocytosis (except macropinocytosis) although whether it involves clathrin or caveolae is not clear at this point.[30] In one of the relevant studies, it was shown that the particles are encapsulated in vesicle systems such as endosomes and subject to the intracellular transport,

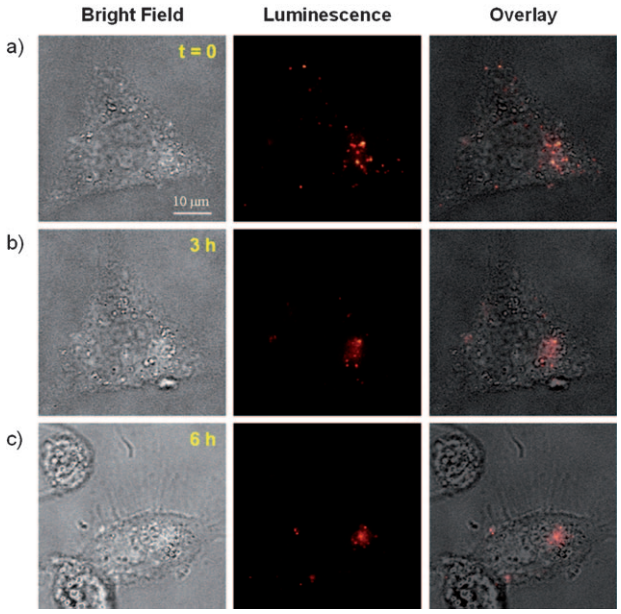

Figure 2. Snapshot images of UCNPs in a single living HeLa cell at a) 0, b) 3, and c) 6 h, adopted from a 6 h long movie taken at 20 frames s^{-1}. Bright-field images of the cell (left panels), luminescence images (middle panels), and overlay images (right panels) are shown. In (c) ($t = 6$ h), cells in the neighborhood happened to move into the field of view (left corners).

which leads to the accumulation of particles at the perinuclear region.[28] Such inhomogeneous particle distribution in the cytoplasm was also observed for UCNPs as in Figure 2. The slight decrease of overall signal at later times (Figure 2c), which we observed frequently in this kind of measurements, is not likely to be due to photobleaching of UCNPs for two reasons: 1) a single UCNP does not exhibit any photobleaching in this timescale according to the previous reports,[20,21] and 2) similar signal loss was observed even when we took snapshot images by exciting the cell sample infrequently with 1 s duration. Instead, we believe that the release of particles out of the plasma membrane via, for example, exocytosis is the reason for the signal loss. It might also be due to chemical degradation of particles by, for example, fusion with lysosomes. Further studies are necessary to elucidate the detailed mechanism underlying such signal loss. Interestingly, we occasionally observed cell divisions while acquiring the data (Figure S4 in the Supporting Information) in which the internalized particles are shared by the daughter cells. This is another piece of evidence that the cells behave normally even under the intense illumination (3 kW cm^{-2}) at 980 nm.

The real-time images visualize the UCNPs moving on the focal plane of the objective. Most of the particles or their aggregates display random spatial fluctuations with relatively low amplitudes, while some of them undergo abrupt directed movements that typically last a few seconds. Such behavior represents intracellular transport of vesicle-encapsulated nanoparticles in the endocytic pathway.[15,28] From the luminescence intensity, we could estimate the number of UCNPs per vesicle, which was broadly distributed from one to three (Methods section and Figure S5 in the Supporting Information). To gain more insights into the dynamics of individual UCNP-containing vesicles, the data were analyzed further by a particle-tracking technique.[31–34] Figure 3a shows a typical result of UCNP tracking in real time (see also Movie S1 in the Supporting Information). The centroid position of a single luminescent spot (i.e., a single UCNP or a small aggregate in a vesicle) in each image frame was determined by fitting the point-spread function to a Gaussian distribution. The localization accuracy was estimated to be 3 nm for the typical UCNP signal level (Methods section in the Supporting Information).[35] Figure 3b shows the displacement traces for the trajectory in Figure 3a. Both the relative displacement of the UCNP-containing vesicles with respect to the starting point and the cumulative distance of the transport were plotted. The trajectory is composed of multiple dynamic phases characterized by distinct transport speed as has been reported previously for different types of nanoparticles.[11,36,37] For example, in the initial part of the trajectory designated as phase I, the UCNP-containing vesicle does not exhibit any significant displacement and apparently fluctuates within a very tiny area. In contrast, the particles are transported along a relatively linear path during phases II, III, and IV at 1.3, 2.1, and 1.1 μm s^{-1}, respectively. In Figure 3c, the mean square displacements (MSDs) are plotted for the phases II, III, and IV. Each MSD plot was well represented by the quadratic function of time intervals (Δt) $\mathrm{MSD} = 4D\Delta t + v^2\Delta t^2$,[31] which suggests that UCNPs were transported actively by intracellular motor proteins walking on the microtubules or

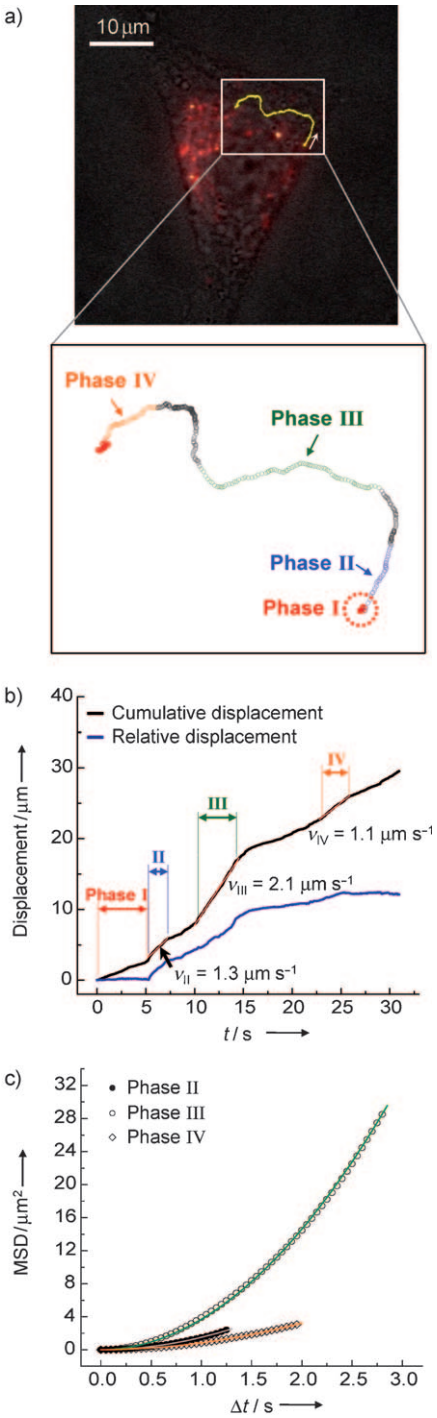

Figure 3. a) Trajectory of a vesicle containing UCNPs transported from the cell periphery to the perinuclear region presumably by dyneins. In phase I, the vesicle is initially confined in a small area. The segments of the trajectory, which display approximately linear paths, are designated as phases II–IV. b) Cumulative and relative displacement traces for the trajectory shown in (a). The transport speeds were calculated for phases II–IV by linear regression. c) MSD plots for phases II–IV. They are all well fit to the equation $\mathrm{MSD} = 4D\Delta t + v^2\Delta t^2$, which is indicative of active transport in two dimensions. The diffusion coefficients (D) were estimated to be 0.016, 0.023, and 0.017 μm^2 s^{-1} for phases II, III, and IV, respectively.

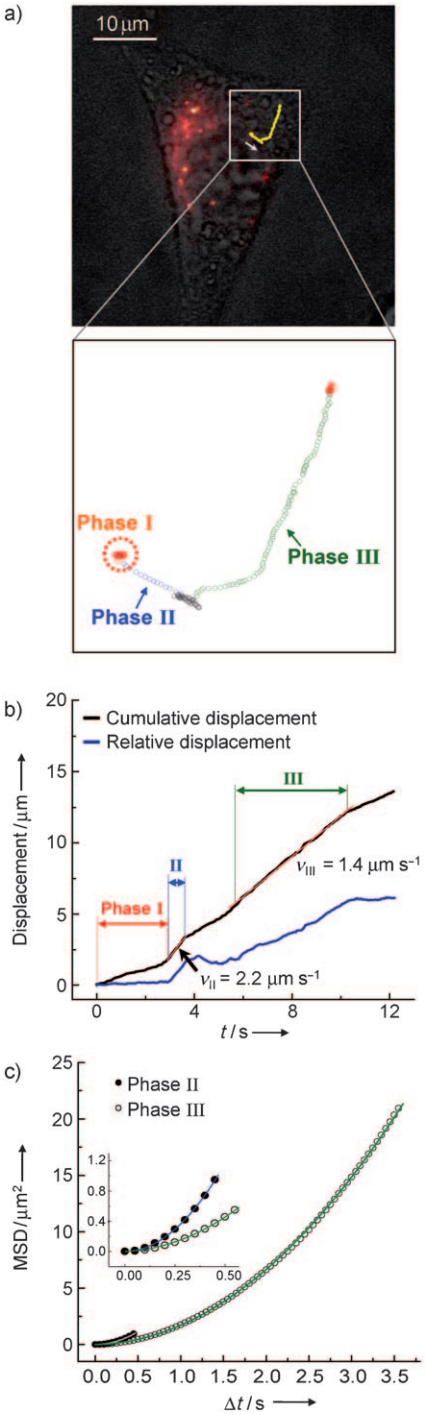

Figure 4. a) Trajectory of a vesicle containing UCNPs transported from the perinuclear region to the cell periphery presumably by kinesins. In phase I, the vesicle is initially confined in a small area. The segments of the trajectory, which display approximately linear paths, are designated as phases II and III. b) Cumulative and relative displacement traces for the trajectory shown in (a). The transport speeds were calculated for phases II and III by linear regression. c) MSD plots for phases II and III. They are well fit to the equation $MSD = 4D\Delta t + v^2\Delta t^2$, which is indicative of active transport in two dimensions. The diffusion coefficients (D) were estimated to be 0.008, 0.024 μm^2 s^{-1} for phases II and III, respectively.

actin filaments.[38] When we treated the cells with nocodazole (30 μM), a drug that inhibits the polymerization of microtubules, no directed transport was observed. In contrast, directed transports were not significantly affected upon treatment with cytochalasin D (5 μM), which disrupts the actin filament network. These results suggest that microtubule-dependent motor proteins such as dyneins and kinesins are responsible for most active transports we observed. Dyneins are known to transport vesicular cargos toward the minus ends of the microtubules near the nucleus, whereas kinesins perform similar tasks in the opposite direction.[38] For the trajectory in Figure 3a, which starts near the cell periphery and proceeds toward perinuclear region, it is likely that dyneins are in action.

We also observed that some particles, initially located at the perinuclear region, were transported away from the nucleus, presumably by kinesins, as shown in Figure 4a (also see Movie S2 in the Supporting Information). In this case, too, we found that multiple distinct phases with characteristic speed constitute the overall trajectory (Figure 4b), and the MSD plot for the directed motion suggests again the operation of active transport (Figure 4c). Interestingly, some UCNP-containing vesicles displayed bidirectional round-trip movements (Figure S6 and Movie S3 in the Supporting Information). This behavior might be simply due to the switching between dyneins and kinesins at the turning point. However, it has also been suggested that a tight coordination of different types of motor proteins might lead to such bidirectional transport.[39]

In summary, we demonstrated the benefits of using UCNPs as the probe for real-time imaging and particle tracking in living HeLa cells. By employing NIR (980 nm) laser as the excitation source, cellular autofluorescence is totally removed, and photoinduced damage is minimized. Combined with the low cytotoxicity and photostability of UCNPs, this method enables uninterrupted long-term imaging of living cells. For the first time, we obtained real-time images of endocytosed UCNPs at the single vesicle level for 6 h continuously at the rate of 20 frames s^{-1}. The dynamics of particle transport was composed of multiple phases within a single trajectory including the active transport by motor proteins such as dyneins and kinesins. Further improvement in the optical upconversion efficiency and surface conjugation schemes will make UCNPs more versatile nanoparticle-based biolabels for intracellular proteins and organelles, accelerating diagnostic and therapeutic applications thereof.

Received: December 17, 2010
Revised: April 5, 2011
Published online: May 13, 2011

Keywords: imaging agents · luminescence · nanoparticles · upconversion

[1] A. P. Alivisatos, *Nat. Biotechnol.* **2004**, *22*, 47.
[2] A. M. Smith, H. Duan, A. M. Mohs, S. Nie, *Adv. Drug Delivery Rev.* **2008**, *60*, 1226.
[3] N. L. Rosi, C. A. Mirkin, *Chem. Rev.* **2005**, *105*, 1547.

[4] A. P. Alivisatos, W. Gu, C. Larabell, *Annu. Rev. Biomed. Eng.* **2005**, *7*, 55.
[5] X. Michalet, et al., *Science* **2005**, *307*, 538. See the Supporting Information.
[6] M. Bruchez, Jr., M. Moronne, P. Gin, S. Weiss, A. P. Alivisatos, *Science* **1998**, *281*, 2013.
[7] M. Nirmal, B. O. Dabbousi, M. G. Bawendi, J. J. Macklin, J. K. Trautman, T. D. Harris, L. E. Brus, *Nature* **1996**, *383*, 802.
[8] J. Yao, D. R. Larson, H. D. Vishwasrao, W. R. Zipfel, W. W. Webb, *Proc. Natl. Acad. Sci. USA* **2005**, *102*, 14284.
[9] A. M. Derfus, W. C. W. Chan, S. N. Bhatia, *Nano Lett.* **2004**, *4*, 11.
[10] O. Faklaris, et al., *ACS Nano* **2009**, *3*, 3955. See the Supporting Information.
[11] B. Zhang, Y. Li, C.-Y. Fang, C.-C. Chang, C.-S. Chen, Y.-Y. Chen, H.-C. Chang, *Small* **2009**, *5*, 2716.
[12] K. Y. Han, K. I. Willig, E. Rittweger, F. Jelezko, C. Eggeling, S. W. Hell, *Nano Lett.* **2009**, *9*, 3323.
[13] N. W. S. Kam, Z. Liu, H. Dai, *Angew. Chem.* **2006**, *118*, 591; *Angew. Chem. Int. Ed.* **2006**, *45*, 577.
[14] H. Jin, D. A. Heller, M. S. Strano, *Nano Lett.* **2008**, *8*, 1577.
[15] H. Jin, D. A. Heller, R. Sharma, M. S. Strano, *ACS Nano* **2009**, *3*, 149.
[16] F. Auzel, *Chem. Rev.* **2004**, *104*, 139.
[17] J. F. Suyver, A. Aebischer, D. Biner, P. Gerner, J. Grimm, S. Heer, K. W. Krämer, C. Reinhard, H. U. Güdel, *Opt. Mater.* **2005**, *27*, 1111.
[18] M. Wang, C.-C. Mi, W.-X. Wang, C.-H. Liu, Y.-F. Wu, Z.-R. Xu, C.-B. Mao, S.-K. Xu, *ACS Nano* **2009**, *3*, 1580.
[19] Z. Li, Y. Zhang, S. Jiang, *Adv. Mater.* **2008**, *20*, 4765.
[20] Y. I. Park et al., *Adv. Mater.* **2009**, *21*, 4467. See the Supporting Information.
[21] S. Wu, G. Han, D. J. Milliron, S. Aloni, V. Altoe, D. V. Talapin, B. E. Cohen, P. J. Schuck, *Proc. Natl. Acad. Sci. USA* **2009**, *106*, 10917.
[22] D. K. Chatterjee, A. J. Rufaihah, Y. Zhang, *Biomaterials* **2008**, *29*, 937.
[23] R. Kumar, M. Nyk, T. Y. Ohulchanskyy, C. A. Flask, P. N. Prasad, *Adv. Funct. Mater.* **2009**, *19*, 853.
[24] F. Wang, et al., *Nature* **2010**, *463*, 1061. See the Supporting Information.
[25] J. V. Frangioni, *Curr. Opin. Chem. Biol.* **2003**, *7*, 626.
[26] R. Weissleder, V. Ntziachristos, *Nat. Med.* **2003**, *9*, 123.
[27] B. D. Chithrani, W. C. W. Chan, *Nano Lett.* **2007**, *7*, 1542.
[28] G. Ruan, A. Agrawal, A. I. Marcus, S. Nie, *J. Am. Chem. Soc.* **2007**, *129*, 14759.
[29] J. B. Delehanty, H. Mattoussi, I. L. Medintz, *Anal. Bioanal. Chem.* **2009**, *393*, 1091.
[30] S. D. Conner, S. L. Schmid, *Nature* **2003**, *422*, 37.
[31] M. J. Saxton, K. Jacobson, *Annu. Rev. Biophys. Biomol. Struct.* **1997**, *26*, 373.
[32] E. Toprak, P. R. Selvin, *Annu. Rev. Biophys. Biomol. Struct.* **2007**, *36*, 349.
[33] F. Pinaud, S. Clarke, A. Sittner, M. Dahan, *Nat. Methods* **2010**, *7*, 275.
[34] V. Levi, E. Gratton, *Cell Biochem. Biophys.* **2007**, *48*, 1.
[35] R. E. Thompson, D. R. Larson, W. W. Webb, *Biophys. J.* **2002**, *82*, 2775.
[36] S. Courty, C. Luccardini, Y. Bellaiche, G. Cappello, M. Dahan, *Nano Lett.* **2006**, *6*, 1491.
[37] X. Nan, P. A. Sims, P. Chen, X. S. Xie, *J. Phys. Chem. B* **2005**, *109*, 24220.
[38] B. Alberts, A. Johnson, J. Lewis, M. Raff, K. Roberts, P. Walter, *Molecular Biology of the Cell*, 5th ed., Garland Science New York, **2008**, pp. 1010–1025.
[39] C. Kural, H. Kim, S. Syed, G. Goshima, V. I. Gelfand, P. R. Selvin, *Science* **2005**, *308*, 1469.

